



Adsorption of thiophene and toluene on NaY zeolites exchanged with Ag(I), Ni(II) and Zn(II)

M.L.M. Oliveira^{a,1}, A.A.L. Miranda^{a,1}, C.M.B.M. Barbosa^{b,2}, C.L. Cavalcante Jr.^{a,1}, D.C.S. Azevedo^{a,*}, E. Rodriguez-Castellon^{c,3}

^aGPSA – Grupo de Pesquisa em Separações por Adsorção, Department of Chemical Engineering, Universidade Federal do Ceará, Campus do Pici, Bl.709, 60455-760, Fortaleza, Brazil

^bLaboratório de Processos Catalíticos, Department of Chemical Engineering, Universidade Federal de Pernambuco, Cidade Universitária, 50740-521 Recife, Brazil

^cDepartment of Inorganic Chemistry, Crystallography and Mineralogy (Associated Unit of ICP-CSIC), Facultad de Ciencias, Universidad de Málaga, Campus Teatinos, 29071 Málaga, Spain

ARTICLE INFO

Article history:

Received 14 November 2008

Received in revised form 30 March 2009

Accepted 14 April 2009

Available online 3 May 2009

Keywords:

Adsorption
Y Zeolite
Thiophene
Nickel
Silver

ABSTRACT

The present study evaluates the adsorption capacity of thiophene and toluene and their competitive behaviour on zeolite NaY exchanged with transition metals (5 wt% Ni, Zn and Ag). The headspace chromatography technique was used to obtain monocomponent apparent adsorption isotherms of thiophene and toluene with NaY, NiY, ZnY and AgY using isooctane as an inert solvent at 30 and 60 °C. Selectivity between toluene and thiophene at saturation capacities were also measured at 30 °C. The adsorption capacity for thiophene increased for the studied adsorbents as follows: NaY < ZnY < NiY < AgY at 30 °C and NaY < NiY < ZnY < AgY at 60 °C. Toluene is less adsorbed, but within the same order of magnitude as thiophene and following the same sorbent order. All adsorbents were moderately selective for toluene. Nevertheless, the sulfur content was successfully reduced in the presence of aromatics and olefins in immersion tests with a model fuel mixture. These results show the importance of inserting transition metals in the zeolitic structure to enhance the adsorption of both aromatic and sulfur containing compounds in organic liquid mixtures, which shows promise to meet environmental standards in transportation fuels.

© 2009 Elsevier Ltd. All rights reserved.

1. Introduction

Sulfur content in transportation fuels (gasoline and diesel) is a significant source of atmospheric pollution by sulfur oxides. Regulations to reduce the sulfur content in automotive diesel to less than 50 ppm have been established in many countries. Sulfur concentrations in the range of 10–50 ppm were to be imposed by 2008 in the US, Europe and elsewhere around the globe [1]. Thus, refiners are facing the challenge of producing increasingly cleaner fuels due to environmental mandates. The hydrodesulfurization process (HDS) is currently used in the petrochemical industry to reduce the contents of undesirable sulfur compounds in hydrocarbon fractions. However, this process is inefficient for the removal of certain types of sulfur compounds, such as thiophene and its derivatives

[2]. Adsorption has been studied as an alternative to sulfur reduction in combination with HDS or replacing it. Moreover, worldwide legislations tend to stipulate reduced levels of aromatics (e.g., benzene and its derivatives), olefins, and oxygenates. Petroleum feedstocks include a wide range of aromatic sulfur containing molecules (e.g., benzothiophene). The conventional hydrodesulfurization (HDS) technologies have limitations in terms of product quality and cost, which are undesirable to refiners [1]. Thiophene (C₄H₄S) and its derivatives are found to be particularly difficult to remove by hydrotreatment processes. Thus, new technological advances are necessary in order to minimize the cost of producing fuels derived from petroleum.

Nanoporous materials with increasingly higher selectivity, such as Y zeolites, have been synthesized and used industrially in the last three decades, both as reaction catalysts [3] or as adsorbents in separation processes [4,5]. More recently, adsorbents containing transition metals (e.g., Ag, Cu, Fe, Ni, Pd and Zn) have been developed for applications in the petrochemical industry [1,2,6–11]. These adsorbents are sulfur-selective for transportation fuels (gasoline, diesel and jet fuel) and they can retain thiophenic compounds by π -complexation bonds. Such bonds are typically

Abbreviations: BJH, Barrer, Jones and Halenda; D–R, Dubinin–Radushkevich; FWHM, full width at half maximum.

* Corresponding author. Tel.: +55 (85) 3366 9611; fax: +55 (85) 3366 9610.

E-mail address: diana@pq.cnpq.br (D.C.S. Azevedo).

¹ Tel.: +55 (85) 3366 9611; fax: +55 (85) 3366 9610.

² Tel.: +55 (81) 21267249; fax: +55 (81) 21268278.

³ Tel.: +34 952131876; fax: +34 952137534.

Nomenclature

b	isotherm equation fitting parameter (L/mol)	q_s	maximum adsorbed phase concentration (mmol/g)
C	sulfur fluid phase concentration (mg/L)	S_{BET}	surface area as determined by BET (Brunauer, Emmet and Teller) method (m^2/g)
C_{eq}	equilibrium fluid phase concentration (mol/L)	$V_{\text{micropore}}$	specific volume of micropores (cm^3/g)
M_L	mass of liquid (mixture) (g)	V_{mesopore}	specific volume of mesopores (cm^3/g)
M_S	mass of solid adsorbent (g)	X	mass fraction in liquid phase dimensionless
n	isotherm equation heterogeneity index dimensionless	Y	mass fraction in vapor phase dimensionless
q	adsorbed phase concentration (mmol/g)		

weaker than chemical covalent bonds, but they are stronger than those involved in physisorption (i.e., van der Waals and electrostatic bonds). A recent work [12] has examined the ability of Cu(II)Y to remove thiophene from various hydrocarbon mixtures at ambient temperature. Adsorption capacity of thiophene decreases substantially when aromatics and/or olefins are present in the feed, suggesting there are competitive interactions of aromatics and thiophenes towards the copper sites. Because aromatics are also undesirable in transportation fuel, an adequate adsorbent should be selective not only to the sulfur compounds, but also to aromatic compounds, such as toluene.

A headspace technique to acquire multicomponent equilibrium data for adsorption from liquid phase was developed back in the eighties and has been more recently applied to mono and multicomponent liquid phase adsorption of xylenes [13,14]. The headspace methodology consists in contacting known quantities of an adsorbent with known quantities of a liquid mixture with defined composition. These are added to a set of headspace vials and allowed to equilibrate at a given temperature [13]. When equilibrium is reached, the vapor phase is sampled and analysed by gas chromatography, the concentration of the liquid phase being calculated from vapor/liquid equilibrium (VLE) relations and the adsorbed phase concentration, by simple mass balance equations. The selectivity of the adsorbent for the components of the studied mixture at saturation capacities may also be determined by the headspace technique, by following the liquid phase composition of a mixture of sorbates in equilibrium with the adsorbent for increasing liquid/solid ratios [14]. The adverse effect of aromatics on the adsorption of sulfur compounds is usually reported in the form of a decrease of the breakthrough or saturation capacity for sulfur [15,16]. The headspace technique has not been reported for such measurements before and it should be particularly useful and straight-forward in the determination of selectivity of two adsorbable components, such as thiophene and toluene. These may be considered as model sulfur and aromatic compounds present in gasoline and light naphtha streams [17]. The choice for thiophene and toluene as key probe-molecules was also based on two factors: their relative volatility (which suits them for the headspace technique under mild temperatures) and their molecular size (which allows them to diffuse easily in faujasite-type materials).

Hence, the main objective of the present study is to report adsorption equilibrium data of thiophene and toluene on the adsorbents NaY, NiY, ZnY and AgY, both as single-component isotherms and their competitive behaviour upon sorbent saturation. Monocomponent liquid phase apparent isotherms for thiophene and toluene were obtained at 30 and 60 °C, considering isooctane as negligibly adsorbed in comparison to aromatic and sulfured compounds [18]. Selectivity between toluene and thiophene at saturation capacities for these adsorbent samples using the headspace technique is reported for the first time. Finally, immersion of the samples in a model fuel sample was performed and the reduction in sulfur content was followed.

2. Experimental section

2.1. Adsorbents preparation

The starting material was a crystalline binderless NaY zeolite (Si/Al = 2.5) in powder form, which was kindly provided by W.R. Grace & Co (Baltimore, USA). The cation-exchanged zeolites (Zn^{2+} , Ni^{2+} and Ag^+) were prepared by ion-exchange from the corresponding metal salt (nitrate) solutions, as reported in the literature [7,15,19]. All transition metal exchanged zeolites (AgY, NiY and ZnY) were to contain about 5 wt% of metal. After exchange, the adsorbents were filtered under vacuum, rinsed with water (28 °C) and dried at 120 °C for 18 h. Then, the exchanged zeolites were calcined at 600 °C, with a heating rate of 2 °C min^{-1} and kept at this temperature for 1 h. Prior to each experiment, the adsorbents were activated at 400 °C for 3 h (heating rate of 2.5 °C min^{-1}), in order to ensure desorption of water and any other substances that could have been previously adsorbed.

2.2. Adsorbents characterization

The prepared samples were characterized by X-ray diffraction (XRD), atomic absorption spectrophotometry (AAS), X-ray photoelectronic spectroscopy (XPS) and N_2 adsorption–desorption isotherms. In order to characterize textural properties of the samples, nitrogen adsorption isotherms at –196 °C were measured in an Autosorb-1 MP apparatus (Quantachrome, USA). Metal content was determined by AAS using a Gemini equipment, model 1475. Powder XRD patterns were registered with a Siemens D500 diffractometer, equipped with a graphite monochromator and using Cu $K\alpha$ radiation. The solids were studied by XPS using a Physical Electronics PHI 5700 spectrometer with non-monochromatic Mg $K\alpha$ 1253.6 eV or Al $K\alpha$ (1486.6 eV) radiations and with a multi-channel detector. Spectra of samples were recorded in the constant pass energy mode at 29.35 eV, using a 720 μm diameter analysis area. Charge referencing was measured using adventitious C 1s signal at 284.8 eV. A PHI ACCESS ESCA-V6.0 F software package was used for data acquisition and data analysis. A Shirley-type background was subtracted from the signals. Recorded spectra were always fitted using Gaussian–Lorentzian curves in order to determine the binding energy of the different element core levels more accurately.

2.3. Adsorption experiments

2.3.1. Monocomponent apparent isotherms for toluene and thiophene

Headspace experiments were performed to measure the monocomponent apparent isotherms of thiophene and toluene on zeolites NaY, NiY, ZnY and AgY at 30 and 60 °C. All reagents were of analytical grade (purity above 99%). Solutions of the sorbate (thiophene or toluene) in isooctane (as inert) at different concentrations (5, 10, 15, 20, 30, 35 and 40 wt%) were placed inside vials together

with known amounts of adsorbent. Vials were sealed and kept in a thermostat bath for 12 h, when equilibrium was assumed to be reached and the vapor phase (in equilibrium with the liquid and solid phases) was sampled and analysed by gas chromatography (Model CP-3800, Varian, USA). By using vapor–liquid equilibrium (VLE) relationships, the liquid phase concentration was determined and, from mass balances, the adsorbed phase concentration of the sorbate (thiophene or toluene) was calculated. Details of the empirical determination of the VLE equation of state may be found in Appendix A.

2.3.2. Selectivity between thiophene and toluene at saturation capacities

To evaluate adsorbent selectivity at saturation, increasing amounts of a binary solution thiophene/toluene (1:1 wt) were placed inside sealed 22-ml vials together with approximately 100 mg of adsorbent. The system was kept at 30 °C for at least ten hours to ensure thermodynamic equilibrium. The vapor phase composition in equilibrium was determined for each vial. When the amount of the added binary solution was enough to completely saturate the adsorbent, the composition of the gas phase would change drastically and reflect the relative preference of the adsorbent for one of the components [13]. Performing experiments with an initially 1:1 wt binary mixture, selectivity, α , may be defined as:

$$\alpha_{\text{thio/tol}} = X_{\text{tol}}/X_{\text{thio}} \quad (1)$$

where X_{tol} and X_{thio} are the mass fractions of toluene and thiophene, in the liquid phase, respectively. Liquid phase composition is determined from the gas phase composition using VLE relations, similarly to the procedure described in Appendix A.

The analysis of the gas phase inside the sealed vials was performed by gas chromatography under the operational parameters and headspace conditions summarized in Tables 1 and 2, respectively. The experimental setup consisted of a Headspace Sampler HP-7000 (Tekmar, USA) connected to a Gas Chromatograph CP-3800 (Varian, USA).

2.3.3. Model fuel measurements

A model gasoline composed of hexane, cyclohexane and toluene (40:40:20 vol) was prepared and doped with approximately 200 ppm of S (thiophene). Each of the adsorbents was put in contact in sealed flasks with a given volume of the model solution (at the dosage of 1 g adsorbent per 10 mL solution) at 30 °C. The sulfur concentration was monitored with time using an X-ray fluorescence analyzer model SLFA 1100H, by Horiba (Ann Arbor, USA).

3. Results and discussion

3.1. Characterization of zeolite samples

Powder diffraction patterns of the zeolites under study are shown in Fig. 1. The similarity in the XRD patterns of the prepared adsorbents as compared to the starting material, NaY zeolite, indicates that the zeolite structure was maintained after ion-exchange. The diffractograms show typical diffraction patterns of the Faujasite framework. In general, the absence of metallic oxides confirms

Table 2
Headspace sampler setup.

Vial volume	22 ml
Vial equilibrium time	240 min
Vial temperature	30 and 60 °C, respectively
Loop temperature	40 and 70 °C, respectively
Transfer line temperature	50 and 80 °C, respectively
Carrier gas pressure	9.3–10.0 psig
Vial pressure	5–10 psig
Time pressure	0.20 min
Loop equilibrium time	0.16 min
Inject time	0.46 min
GC cycle time	10 min

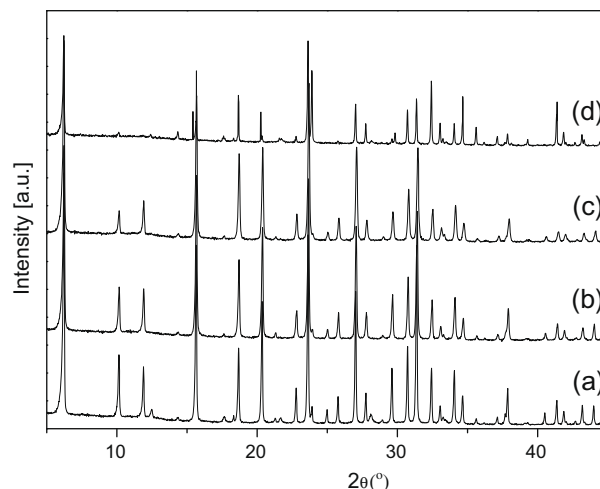


Fig. 1. XRD patterns of the zeolites: (a) NaY, (b) ZnY, (c) NiY and (d) AgY.

the successful incorporation of the metallic cations on the exchange sites of the zeolite. However, for AgY zeolite, a small loss of crystallinity is observed, associated with the lower intensity of the peaks at $2\theta = 10\text{--}12^\circ$ [6,20,21]. This effect could be related to a dealumination of its structure, possibly associated with the location of extra-framework silver.

Nitrogen adsorption isotherms at 77 K are shown for the four solids in Fig. 2. As expected, all of them are type I isotherms, which are typical of microporous solids, with a final upwards tail, due to the presence of a certain amount of mesopores. Ion-exchange by divalent cations and a monovalent large cation (Ag⁺) has the effect

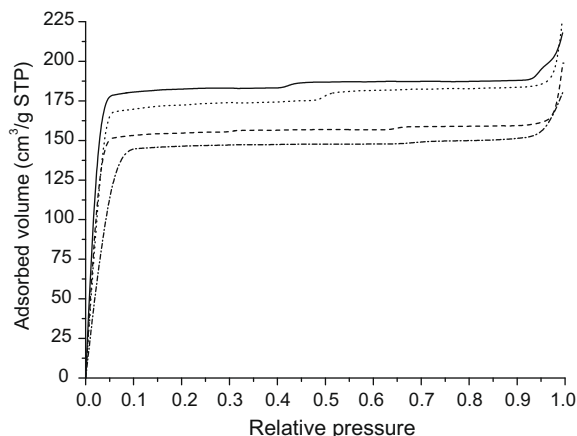


Fig. 2. Nitrogen adsorption isotherms at 77 K for NaY (—), NiY (⋯), ZnY (---) and AgY (-.-).

Table 1
GC operation parameters.

Feature of the experimental device	Value
Column	CP Sil 5 CB, DF = 0.25, 60 m × 0.25 mm
Injector temperature	250 °C
Column oven temperature	80–150 °C
Carrier gas flow rate (N ₂)	1.0 ml min ⁻¹

Table 3
Textural analysis results and metal content of the samples.

Sample	Bulk metal content ^a (wt%)	Surface metal content ^b (wt%)	S_{BET} ($\text{m}^2 \text{g}^{-1}$)	$V_{\text{micropore}}^c$ ($\text{cm}^3 \text{g}^{-1}$)	V_{mesopore}^d ($\text{cm}^3 \text{g}^{-1}$)
AgY	5.25	24.9	393	0.227	0.026
ZnY	4.96	6.01	414	0.243	0.044
NiY	5.31	4.55	494	0.268	0.076
NaY	–	10.43	519	0.270	0.085

^a Determined by AAS.

^b Determined by XPS.

^c Determined by the DR method.

^d Determined by the BJH method.

Table 4
XPS binding energies (eV) of the zeolites. The full width at half maximum (FWHM) of the corresponding signals in eV is included in parenthesis.

Sample	O 1s	Si 2p	Al 2p	Na 1s	Ag 3d _{5/2}	Zn 2p _{3/2}	Ni 2p _{3/2}
NaY	532.2 (2.42)	103.2 (1.99)	74.7 (1.73)	1072.7 (2.08)			
AgY	531.9 (2.34)	102.9 (2.02)	74.7 (1.91)	1072.4 (1.94)	368.7 (1.57)		
ZnY	532.2 (2.36)	103.1 (2.03)	74.7 (1.92)	1072.4 (2.10)		1022.6 (2.16)	
NiY	532.1 (2.28)	102.9 (2.03)	74.6 (2.03)	1072.2 (2.06)			853.4 (23%) 857.1 (77%)

of lowering the horizontal plateaus corresponding to complete micropore filling, meaning that less pore volume is available. Nevertheless, the shape of the isotherm remains the same since the samples maintain their microporous texture. In Table 3, the

textural parameters obtained from N₂ adsorption–desorption isotherms are summarized, together with the metal content of the ion-exchanged zeolites: in the bulk, as determined by AAS and on the surface, as determined by XPS. As cations are incorporated – in the order Ni, Zn and Ag – the metal becomes more concentrated at the surface, possibly causing some pore blocking, which may explain the decreasing S_{BET} and decreasing pore volumes calculated from N₂ isotherms. Ionic radii of the charge-compensating cations used in the ion-exchange may also play a role in the change of textural properties. Whereas Ni²⁺ (0.83 Å) has approximately the same radius as Na⁺ (0.90 Å), the largest Ag⁺ (ionic radius of 1.20 Å) has the most pronounced effect in the structure, which worsens both crystallinity and surface properties.

In addition, XPS has been used to study the nature of the surface species. In Table 4, the binding energies (in eV) of O 1s, Si 2p, Al 2p, Na 1s, Ag 3d_{5/2}, Zn 2p_{3/2} and Ni 2p_{3/2} core levels are summarized for the studied zeolites. According to the XPS data, the Ag 3d_{5/2} binding energy (BE) value (368.7 eV), its narrow FWHM (1.57 eV) – full width at half maximum – and the corresponding kinetic energy of the Auger Ag MNN signal appearing at 350.5 eV are clear indications that silver is present as Ag⁺. The found BE of Ag 3d_{5/2} is close to that reported for Ag₂O (368.4 eV) [22]. The BE value of Zn 3d_{5/2} is 1022.6 eV, which is nearly that of ZnO (1022.5 eV), and the kinetic energy Zn LMN appears at 987.6 eV. This provides evidence that zinc is present as Zn²⁺ [22]. The main Ni 2p_{3/2} signal can be decomposed in two contributions. The most intense, at 857.1 eV, can be associated with Ni²⁺ ions interacting with M–O[–] species. The less intense one, at 853.4 eV, may be assigned to the presence of NiO supported on the zeolitic framework [22,23]. The metal content at the surface is shown in Table 3 and these values

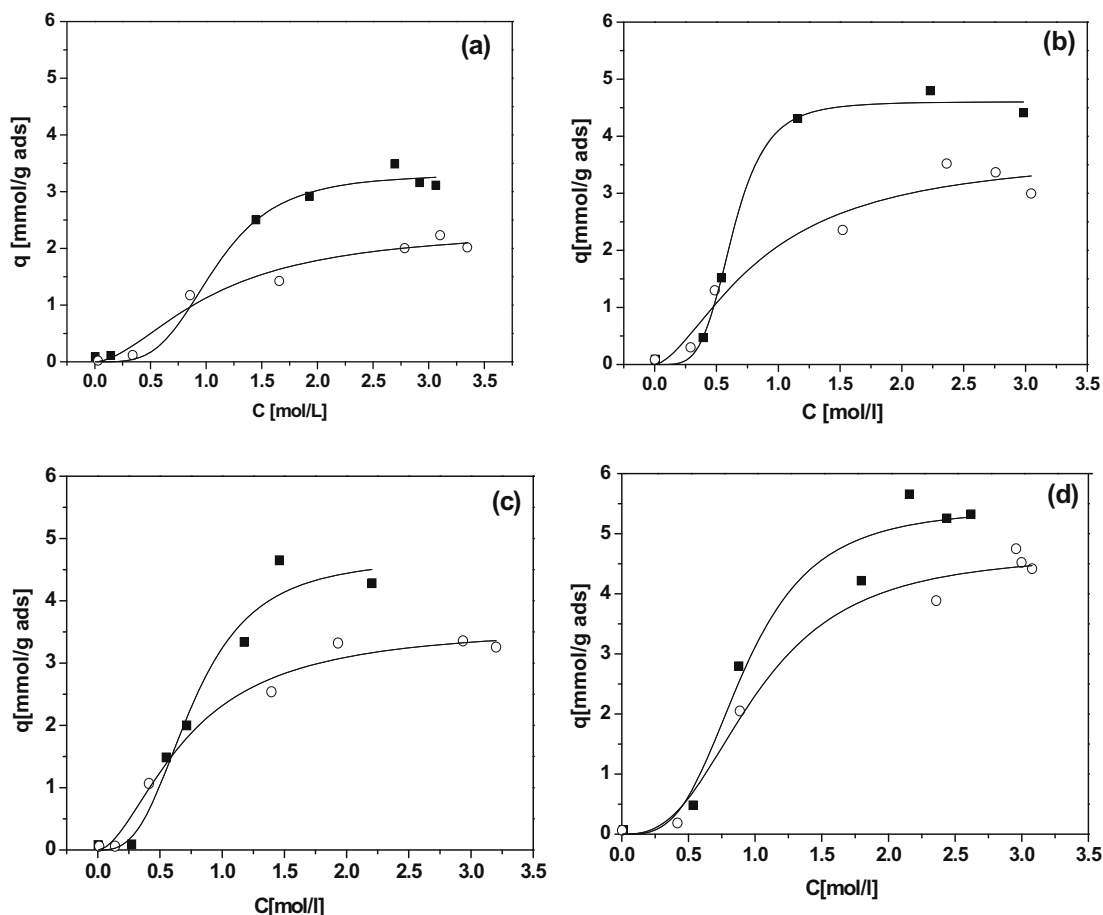


Fig. 3. Thiophene adsorption isotherms at 30 °C (■) and 60 °C (○) by L-F on: (a) NaY; (b) ZnY; (c) NiY and (d) AgY.

are compared to those of the bulk. It is clear that silver is mainly at the surface, another reason that might have caused the decrease in S_{BET} . In the case of Zn, the higher observed content at the surface also produces a decrease of the surface area. However, in the case of nickel, with a surface content lower than that observed in the bulk, the porous properties of the starting zeolite were almost unchanged.

3.2. Thiophene and toluene pseudo-isotherms

The thiophene adsorption pseudo-isotherms over the adsorbents (NaY, ZnY, NiY and AgY) at 30 °C and 60 °C are shown in Fig. 3a–d. The Langmuir–Freundlich (L–F) equation was used to describe the experimental data:

$$\frac{q}{q_s} = \frac{bC_{\text{eq}}^n}{1 + bC_{\text{eq}}^n} \quad (2)$$

where q_s is the maximum adsorption capacity at the experimental temperature, b is a fitting parameter that is related to the adsorbate/adsorbent affinity and n is a heterogeneity index, which will be equal to 1 for a homogeneous material [24]. The adsorbent heterogeneities will be evidenced when the value of n is not unity.

The results show that all adsorption apparent isotherms are unfavourable upto 10 mmol/g, beyond which they become favourable, approaching a plateau (maximum adsorption capacity) asymptotically. In all cases, adsorbed concentrations decrease as temperature increases, which is a typical behaviour of physical reversible adsorption. The highest adsorption capacity for thiophene was found for AgY (ca. 60–90% more than the starting material NaY). Likewise, Yang et al. [6–8] have stated that Ag^+ in the zeolite Y can selectively adsorb sulfur compounds from commercial fuels with high capacity (by π -complexation) at ambient temperature and pressure. Nevertheless, thiophene apparently has different modes of interaction with the proton and cation sites in the Y zeolite. According to Takahashi et al. [9], there is some back-donation of electron charge from the π -orbital of thiophene to the vacant s orbital of the metals known as σ donation. Simultaneously, back-donation of electron charges occurs from the d orbitals of the metals to the π^* orbital (antibonding p orbital) of thiophene, also called π back-donation. In zeolites supporting cations from de d-block (Ag, Zn and Ni), it seems both σ donation and $d-\pi^*$ back-donation are significant, whereas for cation Na^+ , only σ donation mechanism occurs. The equilibrium parameters, as adjusted from the L–F equation, together with the correlation parameter R^2 , are summarized in Table 5 for the four adsorbents. In general, the L–F equation provides a good fit for the measured data. The maximum adsorption capacity lied in the range of 3.32–5.43 mmol S/g for adsorbents tested at 30 °C and 2.37–4.69 mmol S/g at 60 °C. This is in agreement with maximum adsorption capacities reported in the literature [9] for thiophene in vapor phase, as indicated from L–F equation fits, for AgY (3.2 mmol S/g at 120 °C) and NaY (2.68 mmol S/g at 120 °C).

The results of maximum adsorption capacity for NaY are also similar to those obtained by Ng et al. [25] by flow microcalorimetry at 55 °C, using *n*-hexadecane as inert solvent. According to Table 5, the AgY zeolite has the greatest adsorption saturation capacity for thiophene ($q_s = 4.69$ mmol S/g at 60 °C). Hernandez-Maldonado et al. [26] also report the adsorption of sulfur from different fuels by zeolites exchanged with divalent cations, having found that Zn(II) has a lower capacity than Ni(II). Yet both retain sulfur species by $d-\pi^*$ back-donation.

An analogous procedure was performed to measure the equilibrium isotherms of toluene (in isooctane) on the samples under study. The obtained experimental data (not shown) were also fitted by the L–F equation and the respective parameters are

Table 5

Adsorption parameters of thiophene on Y zeolites adjusted by L–F equation.

Zeolite	Temperature (°C)	q_s (mmol S/g)	b (L/mol)	n	R^2
NaY	30	3.32 ± 0.27	0.747	3.79	0.985
	60	2.37 ± 0.46	0.904	1.76	0.955
ZnY	30	4.61 ± 0.12	8.070	4.53	0.994
	60	3.73 ± 0.93	1.253	1.63	0.940
NiY	30	4.70 ± 0.55	2.230	2.97	0.961
	60	3.60 ± 0.32	1.800	1.76	0.984
AgY	30	5.43 ± 0.52	1.348	3.35	0.958
	60	4.69 ± 0.40	0.969	2.72	0.982

Table 6

Adsorption parameters of toluene on Y zeolites adjusted by L–F equation.

Sample	Temperature (°C)	q_s (mmol/g)	b (L/mol)	n	R^2
NaY	30	1.369 ± 0.21	10.064	0.97	0.804
	60	1.256 ± 0.05	12.856	1.16	0.995
ZnY	30	2.940 ± 0.99	2.457	0.78	0.952
	60	2.053 ± 0.11	8.354	1.87	0.969
NiY	30	3.597 ± 5.11	1.133	0.47	0.788
	60	2.770 ± 0.45	1.078	0.73	0.989
AgY	30	3.651 ± 0.564	9.048	1.28	0.865
	60	2.830 ± 0.468	3.224	0.81	0.962

Table 7

Summary of theoretical energies of adsorption [6,24] for thiophene and benzene (in kcal/mol).

	AgY	NiY	ZnY
Thiophene	–21.4	–20.8	–18.7
Benzene	–20.1	–16.7	–17.7

summarized in Table 6. The maximum adsorption capacity q_s is of the same order of magnitude as that of thiophene on a molar basis, which indicates the similar affinity of these materials for both sulfur containing and aromatic substances. Note that the relative error on the estimation of q_s was low enough to conclude that all samples adsorb more thiophene than toluene for pure component measurements. The electron charge provided by the aromatic ring and the electrons available on the d orbitals of Zn(II), Ni(II) and Ag(I) should also enhance both σ donation and $d-\pi^*$ back-donation. The adsorption capacity of the studied zeolites for toluene increases according to this order: NaY < ZnY < NiY < AgY, the same as for thiophene at 30 °C. Their competitive behaviour will be better examined in the next session. Theoretical values for energy of adsorption have been calculated and reported in the literature [6,26] using the Molecular Orbital Theory for zeolites containing the aforementioned cations, considering thiophene and benzene as sorbates. These values are summarized in Table 7. It is expected that toluene follows approximately the behaviour of benzene and, in fact, the relative order of adsorption energy calculated for the thiophene/benzene and the different cations agrees closely with the experimental results found in this work for single-component isotherms.

3.3. Adsorption selectivity between toluene and thiophene

In Fig. 4a–d, the plots for the different adsorbents describe the mass fraction of toluene and thiophene in liquid phase (in equilibrium with the adsorbent) as a function of the liquid/solid mass ratio at 30 °C. Upon saturation, the liquid phase becomes significantly concentrated in thiophene, meaning that all adsorbents preferably adsorb toluene with respect to thiophene. The

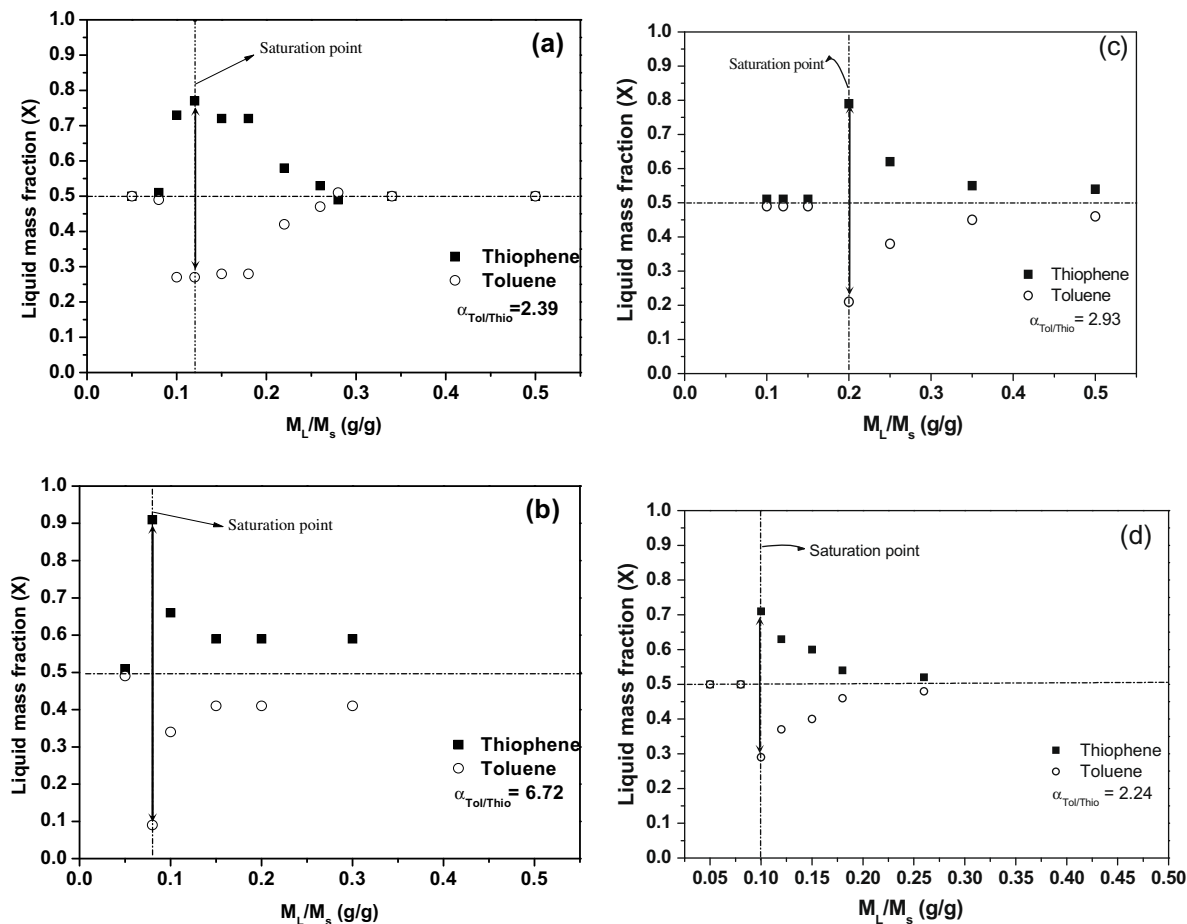


Fig. 4. Selectivity plot for a mixture of toluene and thiophene (1:1 wt) at 30 °C for zeolites: (a) NaY, (b) ZnY, (c) NiY and (d) AgY.

selectivity values reported in each figure were calculated at the saturation point as the ratio between maximum and minimum liquid phase mass fractions, as defined in Eq. (1). This effect is observed at the point where the adsorbent is fully saturated, and an excess of liquid phase has just been formed around the adsorbent sample. Selectivity of toluene with respect to thiophene – the reciprocal of that defined in Eq. (1) – was found to be 2.39; 6.72; 2.93 and 2.24 for NaY, ZnY, NiY and AgY zeolites, respectively, as shown in Fig. 3. Note that the liquid/solid mass ratio at the saturation point varies for each of the four samples. If the micropore volume of each sample was translated into volume of toluene/thiophene mixture (specific mass of 0.959 g cm^{-3}), then a gram of sorbent would have all micropores filled with 0.22–0.26 g of added liquid. From the plots of Fig. 4, the saturation point happens when much less liquid is added, meaning that there may be porous space that is inaccessible to the added liquid mixture. For the cation-exchanged zeolites, NiY is the one that closer approaches this theoretical value, possibly due to the nearly unchanged textural properties.

The competitive adsorption between organic sulfur and aromatics has been reported by some authors as being a crucial factor that affects the adsorption (by π -complexation) of sulfur containing molecules from real fuels [15,26,27]. It is intriguing that, even though the studied samples adsorb more thiophene than toluene in monocomponent measurements, they all preferably adsorb the aromatic under competitive conditions (1:1). This “inversion in selectivity” under competitive conditions has already been observed in simulations for xylenes adsorbed on $\text{AlPO}_4\text{-5}$ and $\text{AlPO}_4\text{-11}$ [28] under a certain composition range. It has been

suggested that it might happen when more than one type of adsorption site is involved, which is the case of cation-exchanged Y zeolites [29,30], and competing species adsorb differently in these distinct sites. On the other hand, the fact that both sulfur and aromatics can be adsorbed may be appropriate if we want to reduce levels of both sulfur and aromatic compounds in transportation fuels to meet environmental standards.

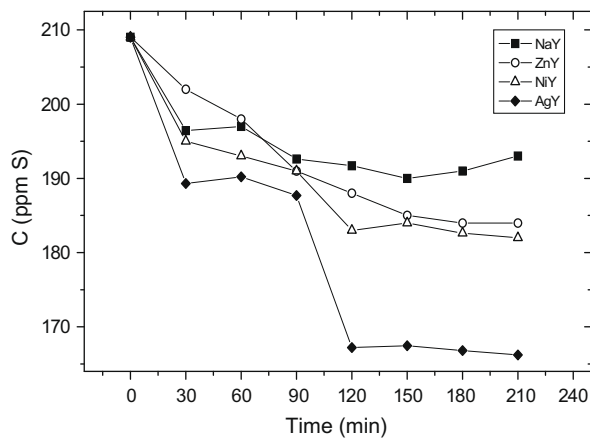


Fig. 5. Decrease in sulfur concentration in a model fuel (hexane/cyclohexane/toluene 40:40:20) in contact with ion-exchanged zeolites. Adsorbent dose = 1 g/10 mL. Temperature = 30 °C.

The decrease in sulfur concentration for a model fuel in contact with the four adsorbent samples at 30 °C is shown in Fig. 5. The apparent adsorption capacity of the samples followed the same order as that found in adsorption pseudo-isotherms of thiophene in isooctane. The best performance was observed in the case of AgY, which was also the sample with lower selectivity towards toluene. As expected, there should be co-adsorption of both toluene and thiophene molecules from a real fuel and the overall reduction in sulfur content will be more or less effective depending on the presence of competing species and on the active metal in π -complexation. If the amount of adsorbed sulfur was calculated by simple mass balance from the data in Fig. 5, these values would range from 4 $\mu\text{mol/S}$ for NaY to 11 $\mu\text{mol/S}$ for AgY, which are considerably below the range of adsorbed concentrations reported in the isotherms (Fig. 3). Nevertheless, given that the distinct decreases in sulfur concentration followed the same trend observed in single-component isotherms, it may be concluded that these ion-exchanged zeolites have potential for adsorptive desulfurization of hydrocarbons despite the presence of competing aromatic species.

4. Conclusions

This study confirms that transition metal (Zn, Ni and Ag) ion-exchanged Y-zeolites have enhanced adsorption properties for thiophene and toluene. The adsorption capacity for both thiophene and toluene in the studied samples followed the order: AgY > NiY > ZnY > NaY. All samples under study adsorb more thiophene than toluene in monocomponent measurements, as indicated by the maximum adsorption capacity estimated from the Langmuir-Freundlich equation. The headspace technique was successfully applied to the determination of thiophene/toluene selectivity upon saturation. All adsorbent samples were moderately selective for toluene with respect to thiophene. Nevertheless, all samples were able to decrease the sulfur content of a model gasoline doped with 200 ppm S. The results indicate that the zeolite sample containing silver (AgY) has the highest capacity for thiophene with a maximum equilibrium load of 5.432 mmol S/g at 30 °C and 4.686 mmol S/g at 60 °C, also showing the least unfavourable selectivity with respect to toluene.

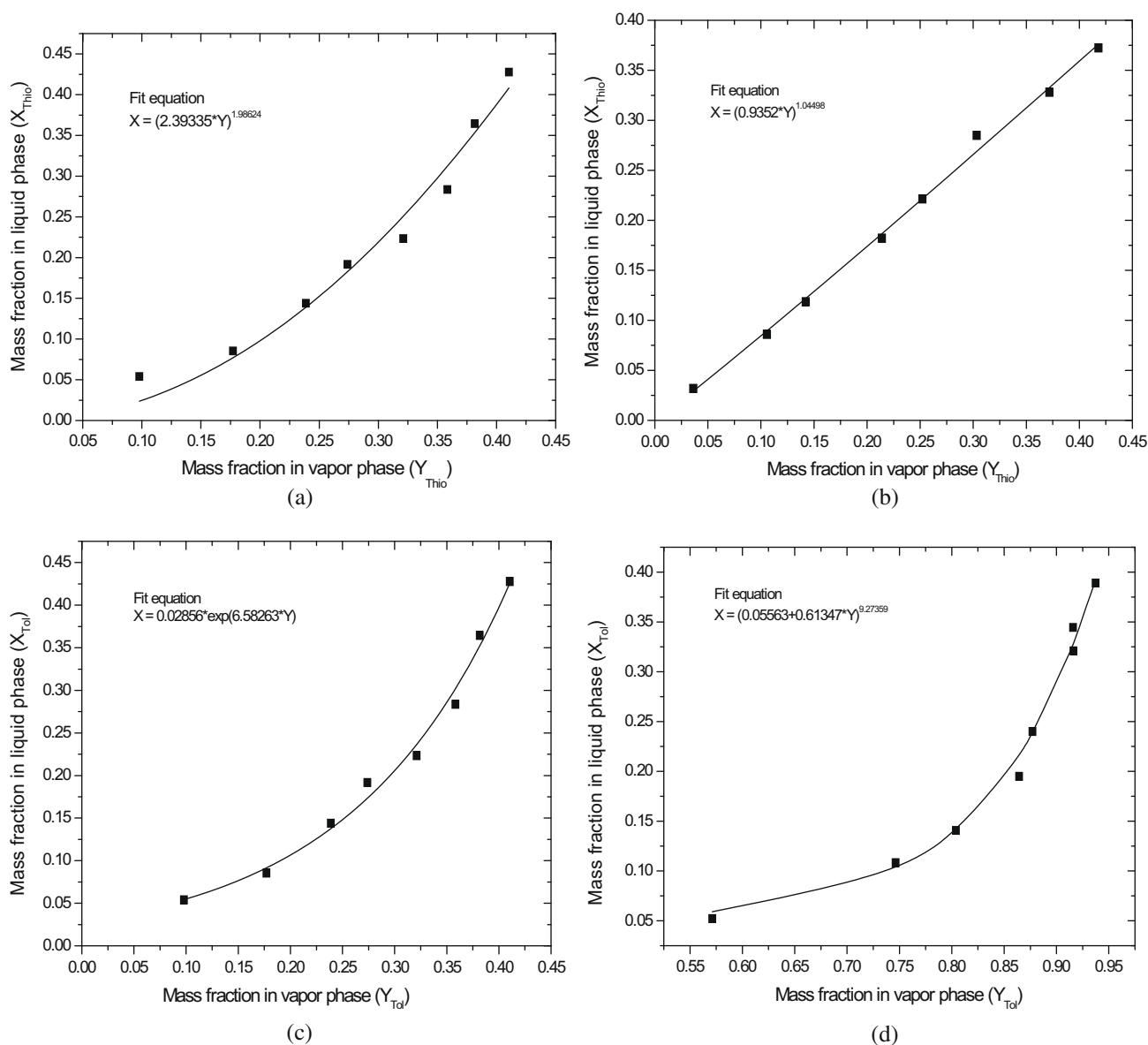


Fig. A1. VLE experimental points and fit equations for thiophene/*n*-octane solutions at (a) 30 °C and (b) 60 °C and toluene/*n*-octane solutions at (c) 30 °C and (d) 60 °C.

Acknowledgments

The authors wish to acknowledge the contribution and support of the following institutions during the course of this research: FINEP/RECAT, ANP – National Petroleum Agency, CNPq (The National Council for Scientific and Technological Development) and CAPES/MECD (Project 084/05). W.R. Grace & Co is gratefully acknowledged for providing NaY zeolite. D.C.S. Azevedo acknowledges financial support from CAPES (proc. 1140/08-8) for a sabbatical leave at the University of Málaga. The authors also thank Dr. S.M.P. Lucena (UFC, Brasil) for the discussion on the phenomenon of “selectivity inversion”.

Appendix A. Determination of empirical equations of state for vapor–liquid equilibria of thiophene/iso-octane and toluene/iso-octane mixtures

VLE empirical correlations were determined by preparing solutions of thiophene/iso-octane and toluene/iso-octane in the concentration range of 10–50 wt%. Each solution was placed in a headspace sealed vial and allowed to equilibrate for 12 h. Samples of the vapor and liquid phases in equilibrium in each vial were analysed and corresponding mass fractions were plotted. Fig. A1 shows the obtained plots and the best equation that fit the data.

References

- [1] Stuntz GF, Plantenga FL. New technologies to meet the low sulfur fuel challenge. *World Petrol Cong Proc* 2002;3:283–95.
- [2] Yang RT. *Adsorbents: fundamentals and applications*. New York: Wiley; 2003.
- [3] Cavalcante Jr CL, Silva NM, Souza-Aguiar EF, Vitor-Sobrinho E. Diffusion of paraffins in dealuminated Y mesoporous molecular sieves. *Adsorption* 2003;9:205–12.
- [4] Cavalcante Jr CL. Industrial adsorption separation processes: fundamentals, modeling and Applications. *Latin Am Appl Res* 2000;30:357–64.
- [5] Cavalcante Jr CL, Azevedo DCS, Souza IG, Silva ACM, Alsina OLS, Lima VE, et al. Sorption and diffusion of p-xylene and o-xylene in aluminophosphate molecular sieve ALPO4-11. *Adsorption* 2000;6:53–9.
- [6] Yang RT, Takahashi A, Yang FH. New sorbents for desulfuration of liquid fuels by π -complexation. *Ind Eng Chem Res* 2001;40:6236–9.
- [7] Yang RT, Yang FH, Takahashi A. New sorbents for desulfuration by π -complexation: thiophene/benzene adsorption. *Ind Eng Chem Res* 2002;41:2487–96.
- [8] Yang RT, Hernandez-Maldonado AJ, Yang FH. Desulfurization of transportation fuels with zeolites under ambient conditions. *Science* 2003;301:79–81.
- [9] Takahashi A, Yang FH, Yang RT. New sorbents for desulfurization by π -complexation: thiophene/benzene adsorption. *Ind Eng Chem Res* 2002;41:2487–96.
- [10] Wang Y, Yang FH, Yang RT, Heinzl JM, Nickens AD. Desulfurization of high-sulfur jet fuel by π -complexation with copper and palladium halide sorbents. *Ind Eng Chem Res* 2006;45:7649–55.
- [11] Wang Y, Yang RT, Heinzl JM. Desulfurization of jet fuel by π -complexation adsorption with metal halides supported on MCM-41 and SBA-15 mesoporous materials. *Chem Eng Sci* 2008;63:356–65.
- [12] King DL, Li L. Removal of sulfur components from low sulfur gasoline using copper exchanged zeolite Y at ambient temperature. *Catal Today* 2006;116:526–9.
- [13] Torres AEB, Neves SB, Abreu JCN, Cavalcante Jr CL, Ruthven DM. Single and multicomponent adsorption equilibrium using headspace chromatography. *Braz J Chem Eng* 2001;18:121–5.
- [14] Buarque HLB, Chivavone OF, Cavalcante Jr CL. Adsorption equilibria of C₈ aromatic liquid mixtures on Y zeolite using headspace chromatography. *Separ Sci Technol* 2005;40:1817–34.
- [15] Bhandari VM, Ko CH, Park JG, Han S-S, Cho S-H, Kim J-N. Desulfurization of diesel using ion-exchanged zeolites. *Chem Eng Sci* 2006;61:2599–608.
- [16] Hernández-Maldonado AJ, Yang RT. Desulfurization of liquid fuels by adsorption via π -complexation with Cu(I)-Y and Ag-Y zeolites. *Ind Eng Chem Res* 2003;42:123–9.
- [17] Song C. An overview of new approaches to deep desulfurization for ultra-clean gasoline, diesel fuel and jet fuel. *Catal Today* 2003;86:211–63.
- [18] Furuya E, Sato K, Kataoka T, Horiguchi T, Otake Y. Amount of aromatic compounds adsorbed on inorganic adsorbents. *Sep Purif Technol* 2004;39:73–8.
- [19] Seidel A, Kampf G, Schmidt A, Boddenberg B. Zeolite ZnY catalysts prepared by solid-state ion exchange. *Catal Lett* 1998;51:213–8.
- [20] Xue M, Chitrakar R, Sakane K, Hirotsu T, Ooi K, Yoshimura Y, et al. Selective adsorption of thiophene and 1-benzothiophene on metal-ion-exchanged zeolites inorganic medium. *J Colloid Interf Sci* 2005;285:487–92.
- [21] Hernandez-Maldonado AJ, Yang RT. Desulfurization of diesel fuels by adsorption via π -complexation with vapor-phase exchanged Cu(I)-Y zeolites. *J Am Chem Soc* 2004;126:992–3.
- [22] Oulder JF, Stickle WF, Sobol PE, Bomben KD. *Handbook of X-ray photoelectron spectroscopy*. Eden Prairie: Perkin-Elmer Corporation; 1992.
- [23] Eliche-Quesada D, Merida-Robles J, Maireles-Torres P, Rodriguez-Castellon E, Jimenez-Lopez A. Hydrogenation and ring opening of tetralin on supported nickel zirconium-doped mesoporous silica catalysts. Influence of the nickel precursor. *Langmuir* 2003;19:4985–91.
- [24] Rudzinski W, Dominko A, Wojciechowski BW. Mixed-gas adsorption on real solid surfaces: lack of correlation between adsorption energies of various components related to the wide applicability of the generalized Langmuir-Freundlich isotherm equation. *Chem Eng J* 1996;64:85–98.
- [25] Ng FTT, Rahman A, Ohasi T, Jiang M. A study of the adsorption of thiophenic sulfur compounds using flow calorimetry. *Appl Catal B: Environ* 2005;56:127–36.
- [26] Hernandez-Maldonado AJ, Yang FH, Qi G, Yang RT. Desulfurization of transportation fuels by π -complexation sorbents: Cu(I)-, Ni(II)- and Zn(II)-zeolites. *Appl Catal B: Environ* 2005;56:111–26.
- [27] Tian F, Wu W, Jiang Z, Liang C, Yang Y, Ying P, et al. The study of thiophene adsorption on to La(III)-exchanged zeolite NaY by FT-IR spectroscopy. *J Colloid Interf Sci* 2006;301:395–401.
- [28] Lucena SMP, Snurr RQ, Cavalcante Jr CL. Monte Carlo and energy minimization studies of binary xylene adsorption in AEL and AFI networks. *Adsorption* 2007;13:477–84.
- [29] Ju S-G, Zeng Y-P, Xing W-H, Chen C-L. Computer simulation of the adsorption of thiophene in all-silica Y and Na-Y. *Langmuir* 2006;22:8353–8.
- [30] Fitch AN, Jobic H, Renouprez A. Localization of benzene in sodium-Y zeolite by powder neutron diffraction. *J Phys Chem* 1986;90:1311–8.